

Research Article

Sm₂FeTaO₇ Photocatalyst for Degradation of Indigo Carmine Dye under Solar Light Irradiation

Leticia M. Torres-Martínez,¹ Miguel A. Ruiz-Gómez,^{1,2} M. Z. Figueroa-Torres,¹
Isaías Juárez-Ramírez,¹ and Edgar Moctezuma²

¹Departamento de Ecomateriales y Energía, Facultad de Ingeniería Civil, Universidad Autónoma de Nuevo León (UANL),
Avenida Universidad S/N, Ciudad Universitaria, 66451 San Nicolás de los Garza, NL, Mexico

²Facultad de Ciencias Químicas, Universidad Autónoma de San Luis Potosí, Avenida Manuel Nava No. 6, 78290 San Luis Potosí,
SLP, Mexico

Correspondence should be addressed to Leticia M. Torres-Martínez, letortres@yahoo.com

Received 15 July 2011; Revised 12 October 2011; Accepted 13 October 2011

Academic Editor: Jae Sung Lee

Copyright © 2012 Leticia M. Torres-Martínez et al. This is an open access article distributed under the Creative Commons Attribution License, which permits unrestricted use, distribution, and reproduction in any medium, provided the original work is properly cited.

This paper is focused to study Sm₂FeTaO₇ pyrochlore-type compound as solar photocatalyst for the degradation of indigo carmine dye in aqueous solution. Sm₂FeTaO₇ was synthesized by using conventional solid state reaction and sol-gel method. X-ray diffraction results indicated that Sm₂FeTaO₇ exhibit a monoclinic crystal structure. By scanning electron microscopy analysis, it was observed that sol-gel material presents particle size of around 150 nm. The specific surface area and energy bandgap values were 12 m² g⁻¹ and 2.0 eV, respectively. The photocatalytic results showed that indigo carmine molecule can be degraded under solar light irradiation using the synthesized materials, sol-gel photocatalyst was 8 times more active than solid state. On the other hand, when Sm₂FeTaO₇ was impregnated with CuO as cocatalyst the photocatalytic activity was increased because CuO acts as electron trap decreasing electron-hole pair recombination rates.

1. Introduction

Nowadays, most of the investigations on photocatalysts are conducted in order to modify the nanostructure to promote their use under visible-light, especially when solar light is used because sun light is an available free energy source [1–5].

Actually, most of the common visible-light-sensitive photocatalysts are binary compounds such as CdS, CdSe, WO₃, TiO₂, ZnO, and Fe₂O₃ that are unstable or have low activity during the photocatalytic process [6–9]. While ternary oxides are a promising family of interesting compounds that can offer the properties desired for an ideal visible-light photocatalyst [10].

Photodegradation using mixed oxides such as A₂BB'O₇ pyrochlore-type compounds has attracted considerable attention because those compounds could be acting as photocatalyst under visible-light irradiation. The slight modification into their crystal structure will cause a variation in their electronic properties provoking an enhancement in the

photocatalytic activity. Those compounds have the advantage that A and B sites can be substituted by several metal ions in order to develop visible responsive photocatalysts.

Previous works reported that pyrochlore containing metal ions like Bi³⁺, Gd³⁺, Sm³⁺, In³⁺, Fe³⁺, Ta⁵⁺, and Sb⁵⁺ improve the photocatalytic activity for dye degradation in aqueous solution under visible-light irradiation. This is because those metals favor the mobility of photoinduced electrons and holes to reach easily the reactive sites on catalyst surface [11–16]. However, to our knowledge, there are no reported studies concerning the photocatalytic activity of pyrochlore compounds under solar light.

Recently in our group, a novel pyrochlore-type compound Sm₂FeTaO₇ has been synthesized with attractive characteristics to be evaluated as potential photocatalyst [17]. For that reason in this paper, the attention is focused to study Sm₂FeTaO₇ as photocatalyst for the degradation of indigo carmine dye in aqueous solution under real and varying solar light illumination. Samples were taken at different times to monitor the progress of the reaction by UV-vis

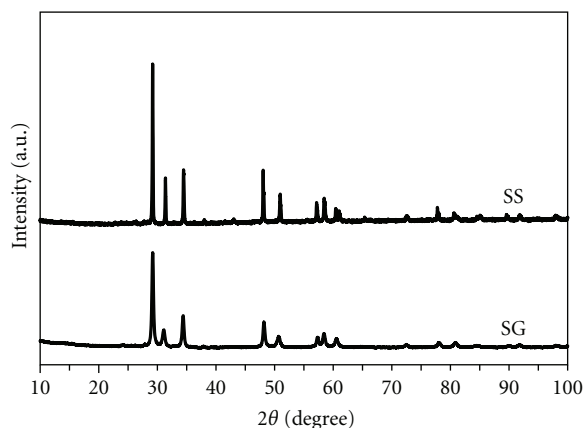


FIGURE 1: X-ray diffraction patterns of $\text{Sm}_2\text{FeTaO}_7$ synthesized by solid state reaction at 1400°C during 36 hours and by sol gel at 800°C during 6 hours [17].

spectroscopy and total organic carbon analysis. Additionally it is proposed the relation between preparative methods and the reaction mechanism of the photocatalytic degradation of indigo carmine dye.

2. Experimental

2.1. Synthesis by Solid State Reaction. $\text{Sm}_2\text{FeTaO}_7$ was obtained by solid state reaction using Sm_2O_3 , Fe_2O_3 and Ta_2O_5 (Aldrich purity >99.9%) as starting materials. The powders were dried at 200°C for 4 hours before the synthesis. Then, stoichiometric amounts of each reactant were perfectly mixed with acetone in an agate mortar. The mixture was ground until complete evaporation of the acetone. This solid was placed into a platinum crucible and calcined at 1400°C for 36 hours under air atmosphere with intermediate regrinding to complete the reaction. The furnace was programmed to reach the calcination temperature at a heating rate of $1^\circ\text{C}/\text{min}$. This sample was labeled as SS.

2.2. Synthesis by Sol-Gel Method. $\text{Sm}_2\text{FeTaO}_7$ was also synthesized by the sol-gel method. In this purpose, a stoichiometric amount of iron (III) acetylacetonate was dissolved in acetylacetonone. The reaction mixture was kept under magnetic stirring for 1 hour and refluxed at 70°C . Then, samarium (III) acetate was dissolved in ethylene glycol and water and refluxed for 1 hour at 70°C . Glacial acetic acid was then added to obtain a colorless samarium solution. At the same time, tantalum ethoxide was mixed with ethanol. Both the samarium and tantalum solutions were slowly added to the iron (III) acetylacetonate solution, and the resulting solution was refluxed at 70°C for 48 hours. After this time, pH was adjusted to 10 using a solution of ammonium hydroxide. Afterwards, the mixture was kept under the same conditions for 48 hours. The final product was dried for 24 hours at 100°C to obtain the fresh sample. The material was heated up to 800°C at a heating rate of $1^\circ\text{C}/\text{min}$ and calcined for six hours under air atmosphere. This sample was labeled as SG.

2.3. Wet Impregnation Method. $\text{Sm}_2\text{FeTaO}_7$ synthesized by both, solid state and sol-gel, was impregnated with 1% CuO

using the stoichiometric amount of an aqueous solution of cupric nitrate hydrate. $\text{Sm}_2\text{FeTaO}_7$ powders and copper solution were mixed and then stirred at 80°C until complete evaporation of the solvent. Then, the materials were thermally treated at 400°C by 1 hour under an air atmosphere using a heating rate of $10^\circ\text{C}/\text{min}$. These samples were labeled as CuO/SS and CuO/SG.

2.4. Characterization. $\text{Sm}_2\text{FeTaO}_7$ materials were characterized by X-ray powder diffraction (XRD) using a Bruker D8 Advance diffractometer and $\text{CuK}\alpha$ radiation ($\lambda = 1.5406 \text{ \AA}$) as the incident X-ray source. XRD data were collected at room temperature from 10 to 100° with a step interval of 0.01° and a counting time of 1s/step.

Morphology of the samples was observed using a JEOL 6490 LV Scanning Electron Microscope (SEM). All samples were stuck to graphite tape and then placed on an aluminum sample holder and located in the SEM chamber. The content of CuO of the impregnated catalysts was determined by energy dispersive X-ray spectroscopy (EDS) analyzing five random zones.

The optical absorption properties of the samples were analyzed in the range of 200–900 nm at room temperature with a UV-vis spectrophotometer (Lambda 35 Perkin Elmer Corporation) equipped with an integrating sphere attachment. The energy bandgap of $\text{Sm}_2\text{FeTaO}_7$ was determined by reflection spectra following the equation [13, 18] $\alpha h\nu = A(h\nu - E_g)^n$. Here, α , ν , A, and E_g are absorption coefficient, light frequency, proportional constant, and bandgap, respectively.

The specific surface area (S_{BET}) was determined by nitrogen adsorption isotherms from the BET method using the Quantachrome NOVA 2000e equipment. The samples were degassed for 3 hours at 300°C prior to the analysis.

2.5. Photocatalytic Activity. The degradation of indigo carmine dye (Indigo-5,5'-disulfonic acid disodium salt) was carried out using a glass container as reactor under solar light irradiation. Four photodegradation experiments were carried out with an indigo carmine solution (10 mg/L). In each of the experiments, 400 mL of the solution were mixed with 400 mg of catalyst (SS, SG, CuO/SS, and CuO/SG) in the glass reactor. The system was allowed to reach adsorption equilibrium under dark conditions. Then, the reactors were placed under solar illumination. In addition, a similar experiment without using any catalyst was also carried out to monitor pure photochemical degradation reactions.

During the experiment, the reaction mixture was kept under stirring. The temperature was controlled at 30°C running cold water on the external surface of the glass reactor. Samples for analysis were taken at different times to monitor the reaction. Each sample was analyzed by UV-vis spectrophotometer (Lambda 35 Perkin Elmer Corporation) and TOC apparatus (TOC-VCSH, Shimadzu Corporation). All tests were carried out simultaneously to ensure identical experimental conditions. Solar irradiation data were obtained from the Environmental Integrated Monitoring System (SIMA) at Monterrey, Nuevo León, México.

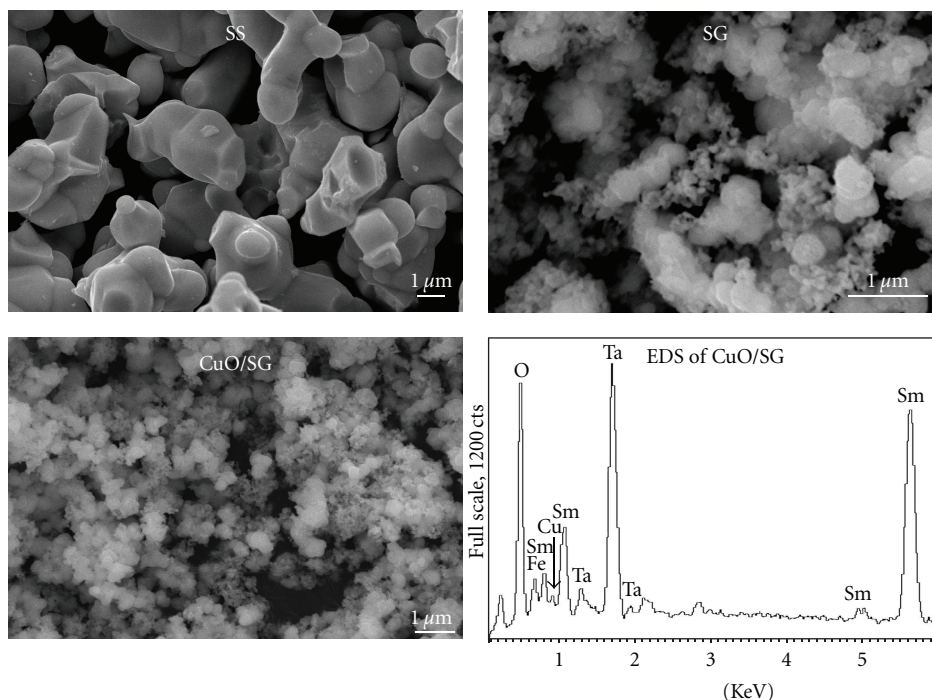


FIGURE 2: SEM images for $\text{Sm}_2\text{FeTaO}_7$ synthesized by solid state and sol gel.

3. Results and Discussion

3.1. Characterization of Pyrochlore-Type

Compound $\text{Sm}_2\text{FeTaO}_7$

3.1.1. X-Ray Diffraction Analysis. $\text{Sm}_2\text{FeTaO}_7$ was obtained as a single phase at 1400°C by solid state reaction and at 800°C by sol-gel method; see Figure 1. This compound crystallized in a monoclinic system with the space group $\text{C}2/c$ [17]. According to XRD patterns both materials showed the same crystal structure but with different crystallinity degree. This result is related to the differences in the synthesis conditions, $1400^\circ\text{C}/36\text{ h}$ and $800^\circ\text{C}/6\text{ h}$ for solid state reaction and sol-gel method, respectively.

Crystal size calculation from the broadening of the main peak ($2\theta = 29.1^\circ$) using the Scherrer formula revealed values of 77 nm for solid state and 43 nm for sol-gel samples. This situation is in agreement with the fact that, by solid state method, material is suffering sintering due to higher thermal treatment than sol-gel, reaching a high crystallization degree.

When CuO/SS and CuO/SG samples were analyzed any XRD peaks attributed to CuO phase were detected since the CuO content in the impregnated catalysts is very low (1 wt.%).

The cell parameters of synthesized compounds are showed in Table 1.

3.1.2. Morphology and Specific Surface Area. Figure 2 shows the morphology of $\text{Sm}_2\text{FeTaO}_7$ synthesized by solid state and sol-gel. It can be seen that morphology and dimensions of particles were strongly dependent on the synthesis route. The particles prepared by solid state reaction have a smooth surface and size of 1 to $4\ \mu\text{m}$ due to the high temperature

TABLE 1: Cell parameters for $\text{Sm}_2\text{FeTaO}_7$ [17].

	$\text{Sm}_2\text{FeTaO}_7$ Solid state 1400°C	$\text{Sm}_2\text{FeTaO}_7$ Sol-gel 800°C
a (Å)	13.1307 (5)	13.0913 (2)
b (Å)	7.5854 (3)	7.5622 (6)
c (Å)	11.6425 (4)	11.7358 (6)
β ($^\circ$)	100.971 (2)	100.933 (4)
Z	8	8

TABLE 2: Physicochemical properties of $\text{Sm}_2\text{FeTaO}_7$ materials.

Sample	CuO (wt. %)	Surface area ($\text{m}^2\ \text{g}^{-1}$)
SS	—	1
SG	—	12
CuO/SS	1.2	1
CuO/SG	1.1	11

of synthesis. While the particles prepared by sol gel have spherical shape and size of around 100 to 150 nm, the micrographs also show these particles are forming aggregates of large size.

Also in Figure 2 are showed the EDS analysis of a specific zone and its respective spectra corresponding to CuO/SG material. The results of this analysis are reported in Table 2.

The results of the BET analysis are also reported in Table 2. $\text{Sm}_2\text{FeTaO}_7$ catalysts prepared by sol-gel had a specific surface area of one order of magnitude higher than the corresponding area of materials prepared by solid state reaction. This result corroborates XRD and SEM analysis, and it was observed that sol-gel material has small particle size. Therefore the highest specific surface area of sol-gel material is due to the soft chemical route used.

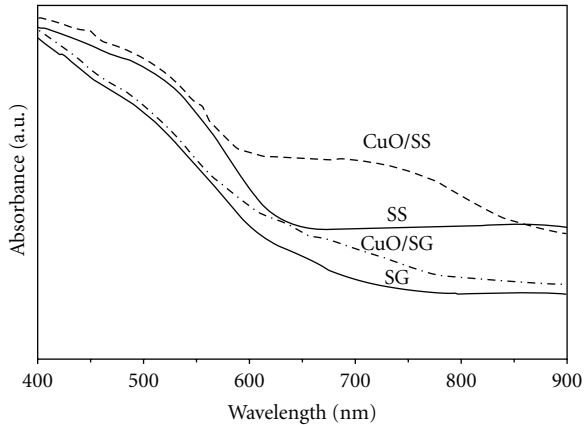
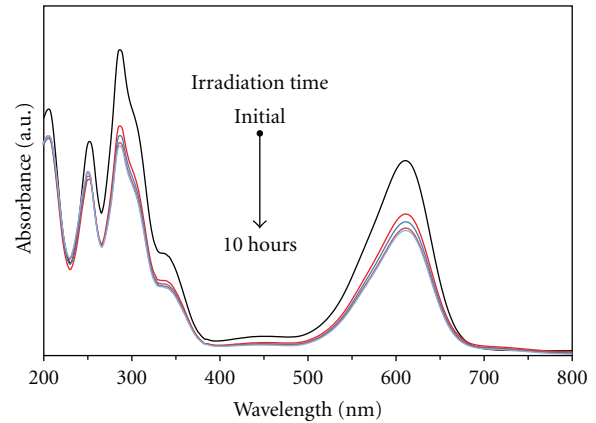
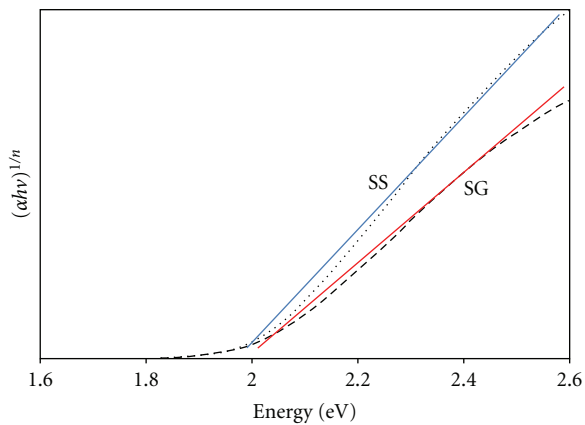
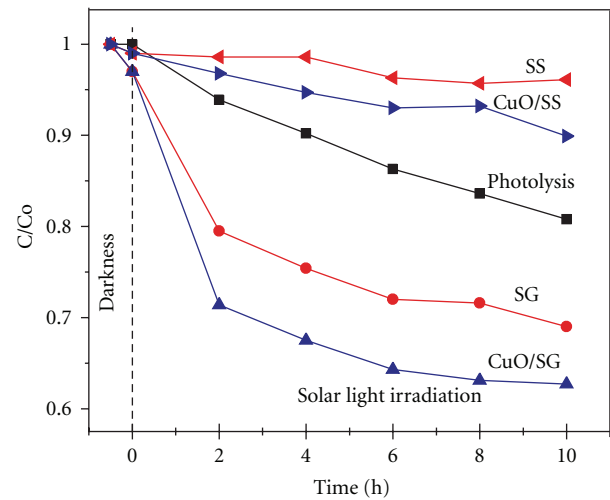
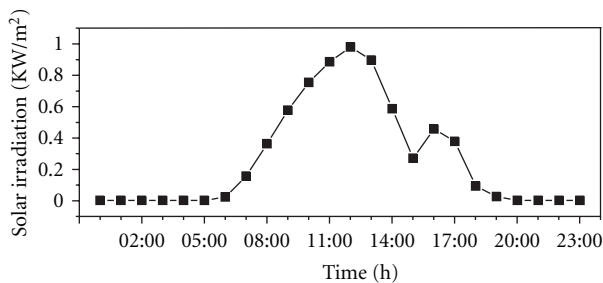
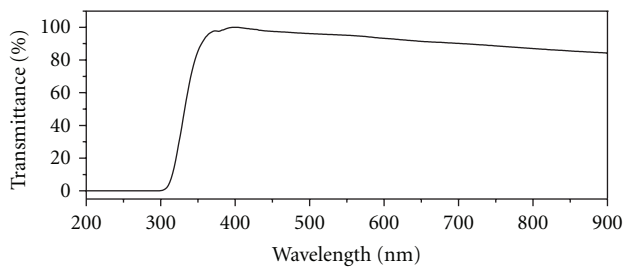
FIGURE 3: UV-vis spectra of $\text{Sm}_2\text{FeTaO}_7$ materials.

FIGURE 6: UV-vis absorption spectra during photodegradation of indigo carmine under solar light irradiation using CuO/SG.

FIGURE 4: Bandgap determination of $\text{Sm}_2\text{FeTaO}_7$.FIGURE 7: Photodegradation of indigo carmine under solar light irradiation using $\text{Sm}_2\text{FeTaO}_7$ and CuO/ $\text{Sm}_2\text{FeTaO}_7$ materials.

(a)



(b)

FIGURE 5: (a) Solar light irradiation conditions during test and (b) percentage of transmittance of the glass container.

In the case of CuO/SS and CuO/SG surface analysis, it is observed that surface area variation after wet impregnation is not significant. Although it is well known that the oxide support nature and metal oxide cocatalyst play an important role in surface area modification [19, 20], it seems that our results are depending on the amount of cocatalyst used.

3.1.3. UV-Vis Analysis. Figure 3 shows the UV-vis spectra for all synthesized samples. It is observed a strong absorption in the visible light region from 400 nm to 900 nm. CuO/SS and CuO/SG showed an additional absorption band at 600–800 nm, which is indicative of the presence of CuO dispersed at the surface [21]. It could be noted that absorption of this band is more evident in CuO/SS sample due to its low surface area, that is, CuO particles are covering much of the available support surface in comparison with CuO/SG.

The bandgap (E_g) of $\text{Sm}_2\text{FeTaO}_7$ synthesized by solid state and sol-gel was determined by the Tauc plot [18] of $(\alpha h\nu)^{1/n}$ versus $h\nu$ showed in Figure 4. The E_g value obtained was 1.99 eV and 2.01 eV for material synthesized by solid

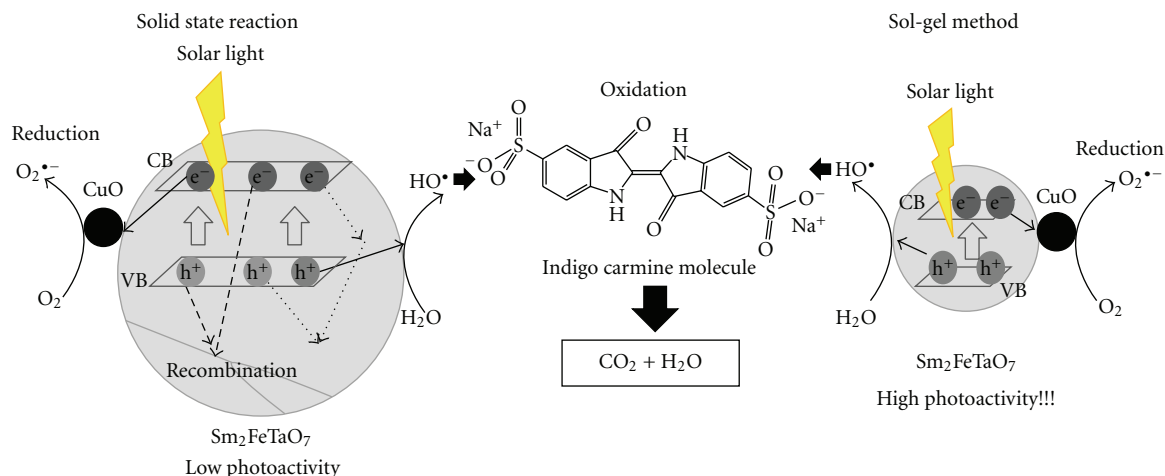


FIGURE 8: Schematic mechanism of the photocatalytic degradation of indigo carmine dye. CB conduction band and VB valence band.

state and sol-gel, respectively. According to Eg results, we assumed that the ability of $\text{Sm}_2\text{FeTaO}_7$ to absorb in the visible light region is directly associated to the presence of Fe. Iron generally acts as electron donor and its 3d electrons are easily excited by the visible light allowing the shift of bandgap to the visible region [10, 16, 22].

3.2. Photocatalytic Evaluation. The photodegradation tests were realized under the solar light irradiation conditions presented in Figure 5(a). Samples were exposed to irradiation from 9:00 AM to 7:00 PM, where the maximum energy was received. Figure 5(b) shows transmittance spectra of glass container used as photocatalytic reactor. It can be noted that the glass container allows the incidence of radiation with wavelength larger 300 nm.

During the photocatalytic experiment, the intensity of the blue color of indigo carmine solution decreased with time. The analysis of the reaction samples by UV-vis spectroscopy shows a slight decrement of all absorption bands (610, 286, 252, and 206 nm). Figure 6 shows the absorption spectra for indigo carmine photodegradation using CuO/SG. It is clear that indigo carmine molecule is suffering degradation under solar light irradiation.

Degradation of indigo carmine solution as a function of irradiation time using the synthesized materials is showed in Figure 7. It can be seen that photolysis reached around 20% due to the small portion of UV light of the solar spectrum, which participate directly in the photochemical reaction, whereas in the presence of the materials synthesized by solid state reaction only 5–10% of degradation is achieved. We can assume that a part of photons are absorbed by materials for the subsequent formation of the electron (e^-) and hole (h^+) pairs limiting the photolysis effect. Besides the photogenerated charges are not participating efficiently for the indigo carmine degradation according to the low activity observed. This fact could be due to several factors such as low interaction between material and dye solution, the low surface area as well as the high rate of the recombination process.

On the other hand, materials synthesized by sol-gel route showed the higher activity for degradation of the aqueous

solution of indigo carmine. In concordance with our results, sol-gel material exhibited an activity 8 times higher than solid state catalyst. It is known that photoactivity is strongly influenced by the nature of material. In our case, sol-gel materials present high surface area and small particle size allowing a better interaction between solution and catalyst material. The presence of small particles provides more active sites and decreases the migration distance of photogenerated electrons and holes promoting the reaction on the catalyst surface [23].

With respect to the use of CuO as cocatalyst promoter, it increases the photocatalytic activity of $\text{Sm}_2\text{FeTaO}_7$. In particular CuO/SG material reached 38% of photodegradation; see Figure 7. In this case CuO acts as an electron trap [24] decreasing the rate of recombination of the photogenerated electron-hole pairs and more holes will be available to oxidize the organic molecules [25]. Additionally, it is known that the recombination competes strongly with the photocatalytic process being it the major limitation in photocatalysis as it reduces the overall quantum efficiency [26].

Additionally, photocatalytic tests were followed by TOC analysis. Results of all samples showed that mineralization is occurring during the reaction. Materials SG and CuO/SG showed 7% and 11% of TOC reduction, respectively, while mineralization for solid state materials is less than 5%.

On basis of the above results, the relation between preparative methods and the reaction mechanism of the photocatalytic degradation of indigo carmine dye is schematically illustrated in Figure 8. It is an attempt to explain why sol gel samples presented higher activity than solid state samples during the photocatalytic process.

In the first step, both CuO/SS and CuO/SG absorb photons with energy greater than their bandgap to form electron-hole pairs. Then, the charge carriers migrate to the surface where redox reactions will occur; simultaneously recombination process is occurring and competes with the photocatalytic process. In our case, both processes are affected by the preparation method. When samples were prepared by sol gel, particle size is smaller than solid state samples; consequently the distance that electrons and holes

have to migrate to the surface becomes short decreasing the recombination rate and providing more active sites for the surface redox reactions. Finally, CuO is acting as electron trap reducing the electron-hole recombination rate, whereas holes are forming oxidative species like hydroxyl radicals that react with indigo carmine dye molecule until forming CO₂ and H₂O [23–25].

According to our results Sm₂FeTaO₇ can be considered as photocatalyst for organic compounds degradation under real and varying solar light illumination as an alternative material for the treatment of wastewater from textile and dyeing industries.

4. Conclusions

The photophysical characteristics of Sm₂FeTaO₇ allowed its use as a visible-light photocatalyst for degradation of indigo carmine dye under solar light irradiation. Its activity was enhanced 8 times when this material was synthesized by sol-gel route due to the high surface area and small particle size compared with solid state material. In addition, the presence of CuO as cocatalyst increases the photocatalytic activity because CuO acts as electron trap avoiding electron-hole pair recombination rates, which favors the oxidation of the indigo carmine molecule.

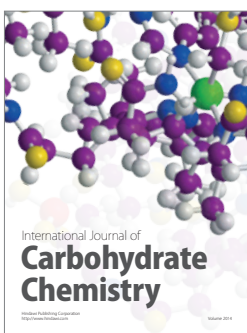
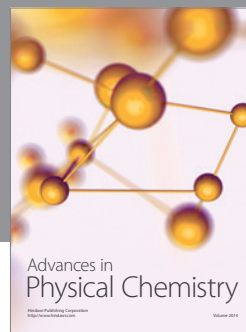
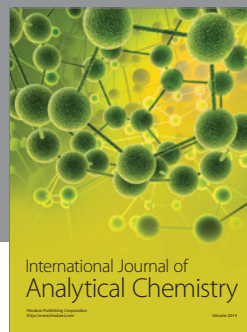
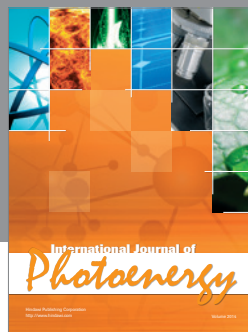
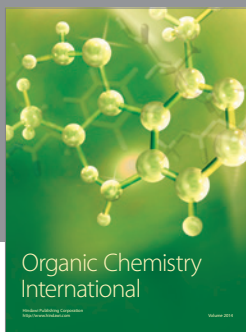
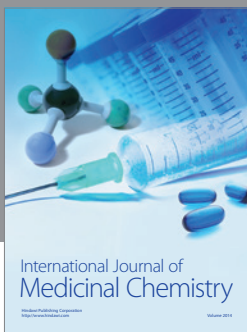
Acknowledgments

Authors want to thank CONACYT for the financial support through the CB-98740-2008, CB-84809-2007, CB-103532-2008 and CB-83923-2007, and PAICYT-UANL2010. Also E. Moctezuma would like to thank to the projects UASLP C10-FRC-07-03. M. Z. Figueroa-Torres thanks CONACYT for financial support through the program A.C.C.I.G.I.-Retención 2010-1 no. 144226. M. A. Ruiz-Gómez thanks CONACYT for Ph.D. scholarship no. 239336.

References

- [1] M. N. Chong, B. Jin, C. W. K. Chow, and C. Saint, "Recent developments in photocatalytic water treatment technology: a review," *Water Research*, vol. 44, no. 10, pp. 2997–3027, 2010.
- [2] J. A. Byrne, P. A. Fernandez-Ibañez, P. S. M. Dunlop, D. M. A. Alrousan, and J. W. J. Hamilton, "Photocatalytic enhancement for solar disinfection of water: a review," *International Journal of Photoenergy*, vol. 2011, Article ID 798051, 12 pages, 2011.
- [3] D. Sánchez Martínez, A. Martínez-De La Cruz, and E. López Cuéllar, "Photocatalytic properties of WO₃ nanoparticles obtained by precipitation in presence of urea as complexing agent," *Applied Catalysis A: General*, vol. 398, no. 1-2, pp. 179–186, 2011.
- [4] G. E. Jonsson, H. Fredriksson, R. Sellappan, and D. Chakarov, "Nanostructures for enhanced light absorption in solar energy devices," *International Journal of Photoenergy*, vol. 2011, Article ID 939807, 11 pages, 2011.
- [5] M. Matsuoka, M. Kitano, M. Takeuchi, K. Tsujimaru, M. Anpo, and J. M. Thomas, "Photocatalysis for new energy production. Recent advances in photocatalytic water splitting reactions for hydrogen production," *Catalysis Today*, vol. 122, no. 1-2, pp. 51–61, 2007.
- [6] M. D. Hernández-Alonso, F. Fresno, S. Suárez, and J. M. Coronado, "Development of alternative photocatalysts to TiO₂: challenges and opportunities," *Energy and Environmental Science*, vol. 2, no. 12, pp. 1231–1257, 2009.
- [7] M. Shao, J. Han, M. Wei, D. G. Evans, and X. Duan, "The synthesis of hierarchical Zn-Ti layered double hydroxide for efficient visible-light photocatalysis," *Chemical Engineering Journal*, vol. 168, no. 2, pp. 519–524, 2011.
- [8] L. S. Roselin and R. Selvin, "Photocatalytic degradation of reactive orange 16 dye in a ZnO coated thin film flow reactor," *Science of Advanced Materials*, vol. 3, no. 2, pp. 251–258, 2011.
- [9] Y. Tokunaga, H. Uchiyama, Y. Oaki, and H. Imai, "Specific photocatalytic performance of nanostructured rutile-type TiO₂: selective oxidation of thiazin dye with a bundled architecture consisting of oriented nanoneedles," *Science of Advanced Materials*, vol. 2, no. 1, pp. 69–73, 2010.
- [10] S. Murugesan, M. N. Huda, Y. Yan, M. M. Al-Jassim, and V. Subramanian, "Band-engineered bismuth titanate pyrochlores for visible light photocatalysis," *Journal of Physical Chemistry C*, vol. 114, no. 23, pp. 10598–10605, 2010.
- [11] J. Luan, W. Zhao, J. Feng et al., "Structural, photophysical and photocatalytic properties of novel Bi₂AlVO₇," *Journal of Hazardous Materials*, vol. 164, no. 2-3, pp. 781–789, 2009.
- [12] J. Luan, M. Li, K. Ma, Y. Li, and Z. Zou, "Photocatalytic activity of novel Y₂InSbO₇ and Y₂GdSbO₇ nanocatalysts for degradation of environmental pollutant rhodamine B under visible light irradiation," *Chemical Engineering Journal*, vol. 167, no. 1, pp. 162–171, 2011.
- [13] J. Luan, K. Ma, B. Pan, Y. Li, X. Wu, and Z. Zou, "Synthesis and catalytic activity of new Gd₂BiSbO₇ and Gd₂YSbO₇ nanocatalysts," *Journal of Molecular Catalysis A: Chemical*, vol. 321, no. 1-2, pp. 1–9, 2010.
- [14] J. Luan, Z. Zheng, H. Cai, X. Wu, G. Luan, and Z. Zou, "Structural characterization and photocatalytic properties of novel Bi₂YVO₈," *Materials Research Bulletin*, vol. 43, no. 12, pp. 3332–3344, 2008.
- [15] J. Luan, H. Cai, X. Hao et al., "Structural characterization and photocatalytic properties of novel Bi₂FeVO₇," *Research on Chemical Intermediates*, vol. 33, no. 6, pp. 487–500, 2007.
- [16] L. L. Garza-Tovar, L. M. Torres-Martínez, D. B. Rodríguez, R. Gómez, and G. del Angel, "Photocatalytic degradation of methylene blue on Bi₂MnBO₇ (M = Al, Fe, In, Sm) sol-gel catalysts," *Journal of Molecular Catalysis A: Chemical*, vol. 247, no. 1-2, pp. 283–290, 2006.
- [17] L. M. Torres-Martínez, M. A. Ruiz-Gómez, M. Z. Figueroa-Torres, I. Juárez-Ramírez, E. Moctezuma, and E. L. Cuellar, "Synthesis by two methods and crystal structure determination of a new pyrochlore-related compound Sm₂FeTaO₇," *Materials Chemistry and Physics*, In press.
- [18] J. Tauc, R. Grigorovici, and A. Vancu, "Optical properties and electronic structure of amorphous germanium," *Physica Status Solidi*, vol. 15, no. 2, pp. 627–637, 1966.
- [19] Y. Chen, H. Yang, X. Liu, and L. Guo, "Effects of cocatalysts on photocatalytic properties of La doped Cd₂TaGaO₆ photocatalysts for hydrogen evolution from ethanol aqueous solution," *International Journal of Hydrogen Energy*, vol. 35, no. 13, pp. 7029–7035, 2010.
- [20] S. M. Saqer, D. I. Kondarides, and X. E. Verykios, "Catalytic activity of supported platinum and metal oxide catalysts for toluene oxidation," *Topics in Catalysis*, vol. 52, no. 5, pp. 517–527, 2009.
- [21] L. S. Yoong, F. K. Chong, and B. K. Dutta, "Development of copper-doped TiO₂ photocatalyst for hydrogen production

- under visible light," *Energy*, vol. 34, no. 10, pp. 1652–1661, 2009.
- [22] T. Umebayashi, T. Yamaki, H. Itoh, and K. Asai, "Analysis of electronic structures of 3d transition metal-doped TiO₂ based on band calculations," *Journal of Physics and Chemistry of Solids*, vol. 63, no. 10, pp. 1909–1920, 2002.
- [23] A. Hagfeld and M. Grätzel, "Light-induced redox reactions in nanocrystalline systems," *Chemical Reviews*, vol. 95, no. 1, pp. 49–68, 1995.
- [24] T. Miwa, S. Kaneco, H. Katsumata et al., "Photocatalytic hydrogen production from aqueous methanol solution with CuO/Al₂O₃/TiO₂ nanocomposite," *International Journal of Hydrogen Energy*, vol. 35, no. 13, pp. 6554–6560, 2010.
- [25] Y. G. Adewuyi, "Sonochemistry in environmental remediation. 2. Heterogeneous sonophotocatalytic oxidation processes for the treatment of pollutants in water," *Environmental Science and Technology*, vol. 39, no. 22, pp. 8557–8570, 2005.
- [26] J. Liqiang, Q. Yichun, W. Baiqi et al., "Review of photoluminescence performance of nano-sized semiconductor materials and its relationships with photocatalytic activity," *Solar Energy Materials and Solar Cells*, vol. 90, no. 12, pp. 1773–1787, 2006.



Hindawi

Submit your manuscripts at
<http://www.hindawi.com>

